ChemComm

COMMUNICATION

View Article Online
View Journal | View Issue

Upconversion fluorescence resonance energy transfer biosensor for sensitive detection of human immunodeficiency virus antibodies in human serum†

Cite this: *Chem. Commun.*, 2014, 50, 4759

Received 22nd January 2014,
Accepted 21st February 2014

DOI: 10.1039/c4cc00569d

www.rsc.org/chemcomm

Yan-Mei Wu, Yao Cen, Li-Jiao Huang, Ru-Qin Yu and Xia Chu*

A facile one-step approach was proposed to prepare hydrophilic and peptide-functionalized upconversion nanoparticles (UCNPs), which were used in the design of a biosensor for the sensitive and selective determination of human immunodeficiency virus antibodies in human serum based on FRET from the UCNPs to the graphene oxide.

Sensitive and selective detection of molecular biomarkers in complex biological samples represents an essential approach in proteomics and clinical diagnostics. Currently, various examples of fluorescence resonance energy transfer (FRET) between emerging nanomaterials and biomolecular recognition units have shown great potential for the development of novel clinical diagnostic techniques.[1] However, traditional downconversion nanomaterials and organic dyes commonly used as donors in the FRET process generally require photoexcitation in the ultraviolet/blue region, in which region the endogenous chromophores in biological or environmental samples can also be excited, leading to strong background fluorescence and thus restricting their applications in complex biological samples.[2]

Lanthanide-doped upconversion nanoparticles (UCNPs), which are capable of emitting strong visible fluorescence under the excitation of near-infrared (NIR) light (typically *ca.* 980 nm), have attracted considerable attention. These UCNPs have proven to exhibit superior features, such as improved quantum yield, tunable multicolor emission, minimal photobleaching, greater light penetration depth in tissue and low toxicity.[3] Most importantly, under the excitation of NIR light, the autofluorescence from biological samples and scattering light become negligible. These merits render UCNPs an ideal candidate as the donor in a FRET-based assay. To date, many research studies have been reported to detect ions,[4] small molecules,[5] protein[6] and nucleic acids[7] based on FRET from UCNPs to various types of acceptors including organic dyes, gold nanoparticles, graphene and carbon nanoparticles.

To develop a UCNPs-based biosensor, a major challenge is to prepare water-dispersible, biocompatible, and functionalizable UCNPs, since they are normally prepared in organic solvents and capped with hydrophobic ligands.[8] Silica coatings formed on the surface of UCNPs have been developed to render the UCNPs dispersible in water, but decreased luminescence intensity and the requirement of further surface modification make this approach undesirable for bioassays.[9] Moreover, although direct synthesis of water-dispersible UCNPs or replacement of hydrophobic ligands with small hydrophilic ligands by ligand exchange could also render UCNPs both water-dispersible and functionalizable,[10] there is still a need for a simple and general method for producing biocompatible UCNPs. Recently, Lu's group reported an approach to engineer a UCNP surface coating with a monolayer of functional phospholipids.[11] Despite the significant advantages, the conjugation of biomolecules with phospholipids with active groups is still required.

Here we developed a facile one-step approach to prepare water-dispersible and peptide-functionalized UCNPs through the self-assembly of phospholipid–peptide conjugation onto the hydrophobic UCNPs surface, and designed a biosensor based on FRET from the peptide-functionalized UCNPs to graphene oxide (GO), a highly efficient energy transfer acceptor.[12] To demonstrate the utility of this strategy, we chose the human immunodeficiency virus (HIV) antibody assay as the model system. HIV is a well-known lentivirus infection of the cells of the human immune system. To date, sensitive and selective determination of HIV antibodies in blood samples is still a challenge due to the high complexity of the sample matrix.

The principle of the upconversion FRET-based biosensor was shown in Scheme 1. An antigenic peptide from HIV type 1 (HIV-1) glycoprotein gp120 immunodominant regions was selected as the recognition unit for the detection of anti-HIV-1 gp120 antibody, and the sequence is as follows: RKRIHIGPGPA-FYTT.[13] A linker sequence KNNNGGG was added to spatially separate the peptide from the nanoparticles and enhance the accessibility to the target HIV antibody. The polypeptide was first

State Key Laboratory of Chemo/Bio-Sensing and Chemometrics, College of Chemistry and Chemical Engineering, Hunan University, Changsha, 410082, P. R. China. E-mail: xiachu@hnu.edu.cn; Fax: +86-731-88821916; Tel: +86-731-88821916

† Electronic supplementary information (ESI) available: Experimental details and supplementary figures. See DOI: 10.1039/c4cc00569d

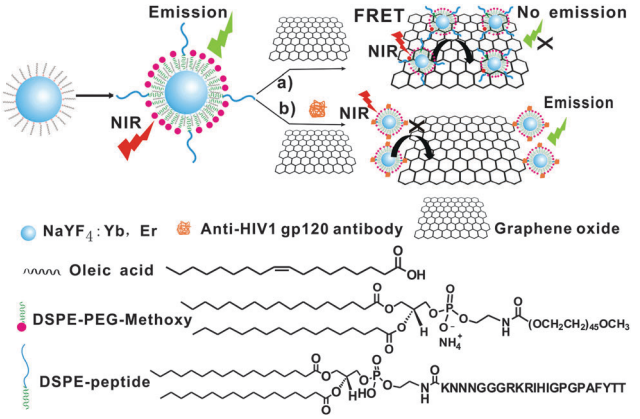

Scheme 1 Schematic illustration of the upconversion FRET-based biosensor for the detection of anti-HIV-1 gp120 antibody.

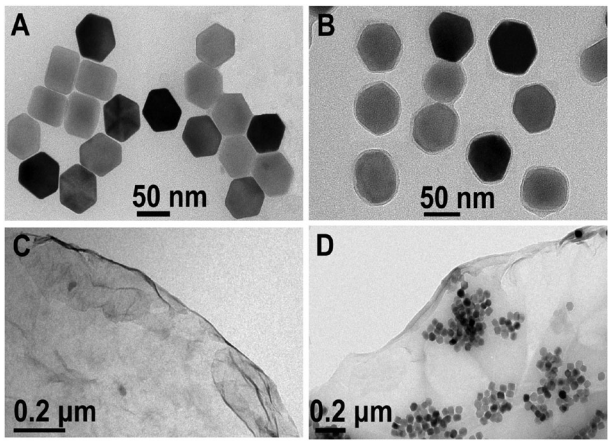

Fig. 1 TEM images of the (A) OA-coated UCNPs in cyclohexane, (B) peptide-functionalized UCNPs in water, (C) as-prepared GO and (D) peptide-functionalized UCNPs–GO complexes in water.

conjugated with the phospholipid to form phospholipid–peptide conjugates, which, as well as PEGylated phospholipids, were then used to prepare the peptide-functionalized UCNPs through a one-step assembly driven by the hydrophobic van der Waals interactions between the hydrophobic tail of the phospholipids and the primary oleate ligands on the UCNP surface. Such a process not only renders these nanocrystals well dispersed in water with excellent stability, but also avoids the conjugation of the peptide with the phospholipid-modified UCNPs. The high flexibility of PEG molecules allows large molecules and nanomaterials to diffuse into the PEG-modified layer to interact with the ligands. When adding GO, peptide-functionalized UCNPs could adsorb on the surface of GO *via* π–π stacking interactions and hydrophobic interactions between the peptides and GO. The upconversion fluorescence could be completely quenched through energy-transfer or electron-transfer processes. In contrast, in the presence of the anti-HIV-1 gp120 antibody, the peptides preferred to bind to their antibody, leading to the formation of peptide–antibody complexes. Therefore the interactions between the peptides and GO would be inhibited, which would keep the UCNPs far away from the GO surface, resulting in a decrease in quenching efficiency and the recovery of upconversion fluorescence.

Highly efficient upconverting $NaYF_4$: Yb, Er nanoparticles were synthesized using oleic acid (OA) as the stabilizing agent. The transmission electron microscopy (TEM) image shows that these nanoparticles display uniform hexagonal plate-like morphology with mean sizes of approximately 60 nm (Fig. 1A). The X-ray diffraction (XRD) analysis agrees well with that of pure hexagonal phase $NaYF_4$ nanocrystals (Fig. S1, ESI†). After functionalization with a mixture of PEGylated phospholipids and phospholipid–peptide conjugation, the resulting lipid–UCNPs show a core–shell structure with a uniform, approximately 2 nm thick, hydrophobic oleic acid–lipid layer around the surface (Fig. 1B and Fig. S2, ESI†). Dynamic light scattering (DLS) measurements indicate that the lipid–UCNPs are well-dispersed in water with a mean hydrodynamic diameter of about 90 nm. In comparison with oleic UCNPs dispersed in cyclohexane (*ca.* 65 nm), this increase of approximately 25 nm in diameter is in agreement with a monolayer of the PEGylated phospholipids (Fig. S3, ESI†).[11] In addition, the FT-IR spectra also demonstrate that the PEGylated phospholipids and phospholipid–peptide conjugation have assembled successfully on the UCNP surface (Fig. S4, ESI†).

Compared with that of OA-coated UCNPs, the peptide-functionalized UCNPs gave a slightly decreased upconversion fluorescence spectrum with two emission bands at 540 and 650 nm respectively, which overlapped with the absorption spectrum of GO as shown in Fig. 2A. The strong fluorescence of peptide-functionalized UCNPs was sufficiently quenched (~90%) after incubation with GO. In contrast, the interaction between GO and UCNPs modified with only PEGylated phospholipids resulted in ~8% fluorescence quenching under identical

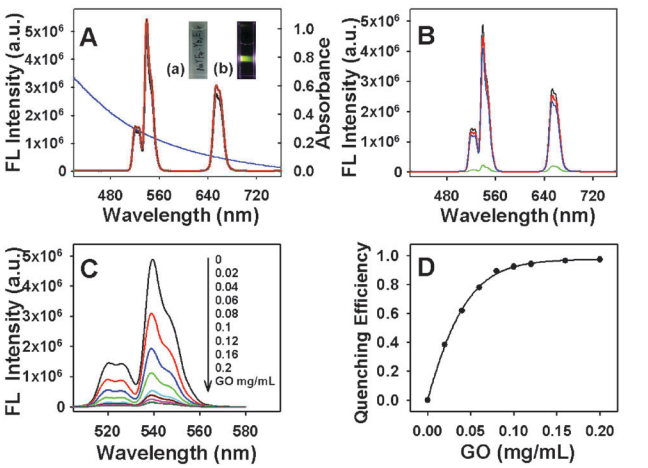

Fig. 2 (A) Upconversion fluorescence spectra of the OA-coated UCNPs (red curve), peptide-functionalized UCNPs (black curve), and the absorption spectrum of GO (blue curve). (The inset shows a photograph of the peptide-functionalized UCNPs in water under ambient light (a) and irradiated by 980 nm light (b).) (B) Fluorescence spectra of peptide-functionalized UCNPs before (black curve) and after (green curve) incubation with GO, and UCNPs modified with only PEGylated phospholipid before (red curve) and after (blue curve) incubation with GO. (C) Fluorescence spectra of peptide-functionalized UCNPs after incubation with various concentrations of GO. (D) Plot of fluorescence quenching efficiency *versus* GO concentration.

conditions (Fig. 2B). This result indicated that the remarkable fluorescence quenching of peptide-functionalized UCNPs was attributed to the selective adsorption of the peptides on the UCNPs onto the GO surface. The TEM image shown in Fig. 1D also confirmed the formation of peptide–UCNPs–GO complexes. The effect of GO concentration on the fluorescence quenching was investigated. As shown in Fig. 2C, the upconversion fluorescence of peptide-functionalized UCNPs was gradually quenched with increasing amounts of GO, and the quenching efficiency reached a plateau when the GO concentration was greater than 80 μg mL^{-1} (Fig. 2D). Therefore, a GO concentration of 80 μg mL^{-1} was selected for the subsequent experiments. In addition, the incubation time of the peptide-functionalized UCNPs with GO was also studied (Fig. S5, ESI†), and an incubation time of 90 min was used in the subsequent experiments.

The detection of anti-HIV-1 gp120 antibodies was then performed. As shown in Fig. S6A, ESI,† the incubation of HIV-1 antibodies and peptide-functionalized UCNPs did indeed result in an increase in fluorescence. In contrast, when human serum albumin was added to replace the antibodies, or the control peptide-modified UCNPs were used, no obvious increase in fluorescence was observed, indicating that the specific interaction between the antigenic peptide and antibody could decrease the adsorption of peptide-functionalized UCNPs on the GO surface. The effect of interaction time between peptide-functionalized UCNPs and antibodies on the fluorescence intensity was investigated (Fig. S7, ESI†), and a reaction time of 90 min was selected. The mole ratio of PEGylated phospholipid to phospholipid–peptide conjugation was also optimized as 9 : 1 in terms of the best signal-to-background ratio (Fig. S8, ESI†). Under the optimal conditions, the upconversion fluorescence intensity increased with increasing antibody concentration (Fig. 3A), and the relative fluorescence intensity was linearly related to the antibody concentration in the range of 5 nM to 150 nM (Fig. 3B). The detection limit of the antibody was calculated to be 2 nM according to the 3σ rule.

To assess the specificity of the upconversion FRET-based biosensor for the target antibody, the responses of the biosensor towards some other proteins were investigated. As shown in Fig. S9, ESI,† the other proteins did not generate significant signals, indicating that other proteins could not interact with the peptide. In addition, the results implied that high concentrations of proteins did not interfere with the binding of peptide-functionalized UCNPs to GO, which may be attributed to the much weaker adsorption of these proteins on GO than that of peptide-functionalized UCNPs to GO due to the multivalent interaction of multiple epitope peptides on the UCNP surface with GO. The results clearly demonstrated the excellent specificity of the biosensor for the target antibody.

To investigate the ability of the upconversion FRET-based biosensor to overcome the interference from background fluorescence and scattering light, we applied the developed biosensor to spiked serum samples. With 10-fold diluted human serum as the assay medium, the same antibody-dependent fluorescence changes as those in aqueous buffer were observed (Fig. S10A, ESI†), except for a slightly increased background. A linear range of 5 to 150 nM was also obtained in the diluted serum (Fig. S10B, ESI†). In addition, a recovery experiment was also performed. Four human serum samples spiked with different concentrations of anti-HIV-1 gp120 antibody were determined, and the results were shown in Table S1, ESI.† The recoveries ranged from 95% to 108% with RSD values of around 6%, which are acceptable for quantitative assays performed in biological samples.

In conclusion, we developed a facile one-step approach to prepare peptide-functionalized UCNPs through the self-assembly of phospholipid–peptide conjugation onto UCNPs surface, and designed a biosensor based on FRET from the peptide-functionalized UCNPs to graphene oxide. The sensor can be used for anti-HIV-1 gp120 antibody sensing both in an aqueous buffer and in a serum matrix with comparable performances, proving that the biosensor is capable of overcoming background interference from complex biological samples. The sensor was applied to determine antibody concentration in human serum with satisfactory results. Owing to the facile fabrication, the sensor could be readily developed to build up sensing platforms for various targets by self-assembly of different peptides to UCNPs.

This work was supported by the National Natural Science Foundation of China (No. 21275045), NCET-11-0121, and Hunan Provincial Natural Science Foundation of China (Grant 12JJ1004).

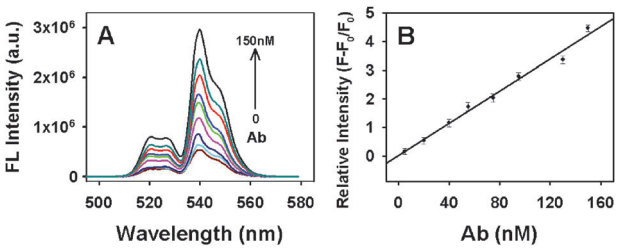

Fig. 3 (A) Upconversion fluorescence spectra of the biosensor with varying concentrations of antibody (0, 5, 20, 40, 55, 75, 95, 130 and 150 nM). (B) Linear relationship between the relative fluorescence intensity and the concentrations of antibody within the range of 5–150 nM. The error bars represented the standard deviations of three independent experiments.

Notes and references

1 (*a*) B. Y. Wu, H. F. Wang, J. T. Chen and X. P. Yan, *J. Am. Chem. Soc.*, 2011, **133**, 686–688; (*b*) S. J. Wu, N. Duan, X. Y. Ma, Y. Xia, Y. Yu, Z. P. Wang and H. X. Wang, *Chem. Commun.*, 2012, **48**, 4866–4868.
2 R. Gill, M. Zayats and I. Willner, *Angew. Chem., Int. Ed.*, 2008, **47**, 7602–7625.
3 M. Haase and H. Schäfer, *Angew. Chem., Int. Ed.*, 2011, **50**, 5808–5829.
4 (*a*) J. L. Liu, Y. Liu, Q. Liu, C. Y. Li, L. N. Sun and F. Y. Li, *J. Am. Chem. Soc.*, 2011, **133**, 15276–15279; (*b*) Q. Liu, J. J. Peng, L. N. Sun and F. Y. Li, *ACS Nano*, 2011, **5**, 8040–8048.
5 (*a*) H. S. Mader and O. S. Wolfbeis, *Anal. Chem.*, 2010, **82**, 5002–5004; (*b*) C. H. Liu, Z. Wang, H. X. Jia and Z. P. Li, *Chem. Commun.*, 2011, **47**, 4661–4663; (*c*) D. E. Achatz, R. J. Meier, L. H. Fischer and O. S. Wolfbeis, *Angew. Chem., Int. Ed.*, 2011, **50**, 260–263; (*d*) S. J. Wu, N. Duan, X. Y. Ma, Y. Xia, H. X. Wang, Z. P. Wang and Q. Zhang, *Anal. Chem.*, 2012, **84**, 6263–6270.
6 (*a*) Y. H. Wang, L. Bao, Z. H. Liu and D. W. Pang, *Anal. Chem.*, 2011, **83**, 8130–8137; (*b*) Y. H. Wang, P. Shen, C. Y. Li, Y. Y. Wang and Z. H. Liu, *Anal. Chem.*, 2012, **84**, 1466–1473.
7 (*a*) P. Zhang, S. Rogelj, K. Nguyen and D. Wheeler, *J. Am. Chem. Soc.*, 2006, **128**, 12410–12411; (*b*) L. Y. Wang and Y. D. Li, *Chem. Commun.*, 2006, 2557–2559.
8 F. Wang, R. R. Deng, J. Wang, Q. X. Wang, Y. Han, H. M. Zhu, X. Y. Chen and X. G. Liu, *Nat. Mater.*, 2011, **10**, 968–973.

9 Z. Q. Li, Y. Zhang and S. Jiang, *Adv. Mater.*, 2008, **20**, 4765–4769.
10 (*a*) F. Wang and X. G. Liu, *J. Am. Chem. Soc.*, 2008, **130**, 5642–5643; (*b*) H. Schäfer, P. Ptacek, K. Kömper and M. Haase, *Chem. Mater.*, 2007, **19**, 1396–1400.
11 L. L. Li, R. Zhang, L. Yin, K. Zheng, W. Qin, P. R. Selvin and Y. Lu, *Angew. Chem., Int. Ed.*, 2012, **51**, 6121–6125.
12 (*a*) Y. Wang, Z. H. Li, D. H. Hu, C. T. Lin, J. H. Li and Y. H. Lin, *J. Am. Chem. Soc.*, 2010, **132**, 9274–9276; (*b*) D. Chen, H. B. Feng and J. H. Li, *Chem. Rev.*, 2012, **112**, 6027–6053; (*c*) Y. Wang, Z. H. Li, J. H. Li and Y. H. Lin, *Trends Biotechnol.*, 2011, **29**, 205–212.
13 C. H. Lu, J. Li, X. L. Zhang, A. X. Zheng, H. H. Yang, X. Chen and G. N. Chen, *Anal. Chem.*, 2011, **83**, 7276–7282.

